

Growth and spreading of quantum resources under random circuit dynamics

Sreemayee Aditya  ^{1,*} Xhek Turkeshi  ^{1,†} and Piotr Sierant  ^{2,‡}

¹*Institut für Theoretische Physik, Zülpicherstraße 77a, 50937, Köln, Germany*

²*Barcelona Supercomputing Center Plaça Eusebi Güell, 1-3 08034, Barcelona, Spain*

Quantum many-body dynamics generate nonclassical correlations naturally described by quantum resource theories. Quantum magic resources (or nonstabilizerness) capture deviation from classically simulable stabilizer states, while coherence and fermionic non-Gaussianity measure departure from the computational basis and from fermionic Gaussian states, respectively. We track these resources in a subsystem of a one-dimensional qubit chain evolved by random brickwall circuits. For resource-generating gates, evolution from low-resource states exhibits a universal rise-peak-fall behavior, with the peak time scaling logarithmically with subsystem size and the resource eventually decaying as the subsystem approaches a maximally mixed state. Circuits whose gates do not create the resource but entangle neighboring qubits, give rise to a ballistic spreading of quantum resource initially confined to a region of the initial state. Our results give a unified picture of spatiotemporal resource dynamics in local circuits and a baseline for more structured quantum many-body systems.

Introduction.— Non-classical features of quantum states such as entanglement [1, 2], anticoncentration [3–7], and the formation of unitary designs [8–14] have become central diagnostics of quantum computational power beyond classical simulability [15–17]. Quantum resource theories [18] of entanglement [1, 2], nonstabilizerness [19–24], coherence [25–27], and bosonic [28, 29] or fermionic [30–34] non-Gaussianity provide a unified framework to quantify such non-classicality, which underpins fault-tolerant quantum computation as well as metrological and thermodynamic advantages. In many-body dynamics, quantum resources track the complexity of states generated by time evolution, providing a lens on quantum chaos [35–37], information scrambling [38–43], thermalization [44–52], properties of ground and critical states [53–57], conformal field theories [58–60], monitored systems [61–64], and metrological responses [65].

Capturing the dynamical behavior of quantum resources in many-body settings typically requires computing nonlinear resource measures (or monotones) [18, 66]. Random quantum circuits [67–70] provide minimally structured models of local quantum dynamics and have yielded a detailed understanding of entanglement growth via the minimal-membrane picture [71–76] and information scrambling [68, 77]. Recent work has extended this analysis to coherence [78–84] and nonstabilizerness [85], showing that these resources saturate on timescales scaling only logarithmically with system size, much faster than the system-size-linear saturation of entanglement entropy. While ergodic Floquet models exhibit analogous phenomenology, local Hamiltonian dynamics yields a parametrically slower resource growth [86].

Most of these works, however, focus on *global* resource measures, such as the stabilizer entropy [21] or participation entropy [87–96] of the full many-body state. Global metrics quantify how much resource the system carries overall, but do not track its distribution and propagation. Fault-tolerant architectures, however, require logical operations that spread errors only locally, e.g., via ge-

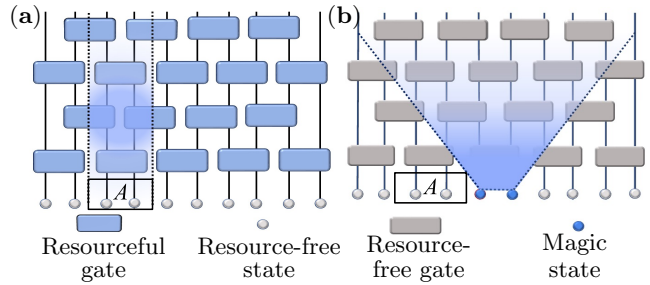


Figure 1. Our setup. (a) *Local resource dynamics*: We track the resource content of a subsystem A under brickwall circuit dynamics with resource-generating gates starting from a resource-free initial state, uncovering a universal rise-peak-fall profile. (b) *Resource spreading*: Starting from an initial state where the resource is confined to a small region and evolving with circuits whose gates do not generate the resource, we scan the spatiotemporal position of A and expose ballistic spreading of the resource.

ometrically local gates [97–99]. Local resource spreading can also underlie the quantum Mpemba effect [100–103]. Hence, for understanding information scrambling, thermalization, and experimentally relevant local probes, the *local* structure of quantum resource growth is the key.

In this Letter, we study the *local dynamics* of quantum resources in one-dimensional random brickwork circuits, focusing on three paradigmatic resources: nonstabilizerness, coherence, and fermionic non-Gaussianity. We consider a subsystem A and analyze two complementary setups, see Fig. 1. In the first setup, circuits are composed of random, resource-generating two-qubit gates acting on an initial computational-basis product state. This allows us to characterize *local resource dynamics*, from the initial buildup induced by the gates to the subsequent decay of the resource content of A as it approaches a maximally mixed state. In the second setup, we consider circuits whose gates do not generate the resource, acting on an initial state where the resource is localized in a finite region. By shifting the position of A , we reveal ballistic

spreading of the initially localized resourceful cluster.

Quantum resources.— Resource theories provide a general framework for quantifying nonclassical features of quantum states by distinguishing a set of *free states*, which can be prepared without cost, and *free operations*, which do not generate the resource from free states. Any state outside the free set is deemed resourceful. This naturally leads to definition of monotones $M(\rho)$, i.e., functions of state ρ of L qubits that satisfy two basic requirements: (i) *faithfulness* — $M(\rho) = 0$ if and only if ρ is a free state, and (ii) *monotonicity* — $M(\Lambda[\rho]) \leq M(\rho)$ for all free operations Λ .

Stabilizer states, denoted as $|\sigma\rangle$, are pure states obtained from $|0\rangle^{\otimes L}$ by action of Clifford unitaries, i.e., operators that map a Pauli string (an L -fold tensor product of Pauli operators I, X, Y, Z) to a Pauli string. In the resource theory of nonstabilizerness the *free states* belong to the convex hull $\text{STAB} = \{\sum_i p_i |\sigma_i\rangle\langle\sigma_i| : p_i > 0, \sum_i p_i = 1\}$ of pure stabilizer states. The *free operations* are stabilizer protocols [104], that include action of Clifford unitaries. Stabilizer entropy [105], is an experimentally relevant [106–109] measure of nonstabilizerness, which, however, has the monotonicity property only for pure states [104, 105]. Since we aim at quantifying nonstabilizerness of a subsystem A consisting of L_A qubits that is generally in a mixed state ρ_A , we utilize the log-robustness of magic (LRoM) [24, 110, 111] defined as

$$\mathcal{L}(\rho_A) = \log \min_{x_1, \dots, x_k} \left\{ \sum_{i=1}^k |x_i| : \rho_A = \sum_{i=1}^k x_i \sigma_i, \right\}, \quad (1)$$

where k is an integer. The LRoM quantifies the distance of ρ_A from STAB and is a faithful monotone of the resource theory of nonstabilizerness.

Coherence is at the heart of interference phenomena. In the theory of quantum coherence, one distinguishes a specific basis, chosen here as the computational basis $\mathcal{B} = \{|i\rangle\}_{i=1, \dots, 2^L}$ and selects the set of *free states* as the convex hull $\text{INCOH} = \{\sum_i p_i |i\rangle\langle i| : p_i > 0, \sum_i p_i = 1\}$, referred to as the incoherent states. *Free operations* in the theory of coherence [25, 112] are not able to create coherence from the incoherent states, and the relative entropy of coherence [25–27, 112],

$$C_d(\rho_A) = S(\rho_A^D) - S(\rho_A), \quad (2)$$

where $S(\rho) = -\text{tr}(\rho \log_2 \rho)$ is the von Neumann entropy and $\rho_A^D = \sum_z (z|\rho_A|z)\langle z|$, is a faithful monotone of coherence of the subsystem A .

Fermionic Gaussian states are of the form $\rho_G = c \exp(\frac{i}{2} \sum_{mn} g_{mn} \gamma_m \gamma_n)$ [113, 114], where $\gamma_{2k-1} = (\prod_{m=1}^{k-1} Z_m) X_k$, $\gamma_{2k} = (\prod_{m=1}^{k-1} Z_m) Y_k$ are known as Majorana operators, and coefficients g_{mn} form an antisymmetric $2L \times 2L$ matrix while c is a constant. In the resource theory of fermionic non-Gaussianity $\text{GAUSS} = \{\rho_G\}$ is the set of *free states*, while *free operations* include fermionic Gaussian unitaries, i.e. operators of the

form $U_G = \exp(\frac{1}{2} \sum_{mn} h_{mn} \gamma_n \gamma_m)$. A faithful monotone of fermionic non-Gaussianity is the relative entropy of non-Gaussianity [31, 32]

$$\mathcal{NG}(\rho_A) = S(\rho_A^F) - S(\rho_A), \quad (3)$$

where ρ_A^F is a fermionic Gaussian state with the covariance matrix $\Gamma_{ab} = -\frac{i}{2} \text{tr}[\rho_A(\gamma_a \gamma_b - \gamma_b \gamma_a)]$. The von Neumann entropy of ρ_A^F is evaluated with the techniques for free-fermions [115] as $S(\rho_A^F) = \sum_{j=1}^{L_A} H\left(\frac{1+\lambda_j}{2}\right)$, where λ_j are the Williamson eigenvalues [116, 117] of the covariance matrix Γ_{ab} and $H(x) = -x \log_2 x - (1-x) \log_2(1-x)$.

Random circuits.— We consider a one-dimensional chain of L qubits, see Fig. 1, evolving under brick-wall circuit. The evolution operator reads $U_t = \prod_{r=1}^t U^{(r)}$, where t is the circuit depth, referred to as time. The layers $U^{(r)}$ of the circuits are fixed as

$$U^{(2m)} = \prod_{i=1}^{N/2-1} u_{2i, 2i+1}, \quad U^{(2m+1)} = \prod_{i=1}^{N/2} u_{2i-1, 2i}, \quad (4)$$

where each two-qubit gate $u_{i,j}$ is drawn with probability ϵ from an ensemble (depending on the setup and resource) and is the identity $\mathbb{1}_{i,j}$ with probability $1-\epsilon$. The dilution parameter ϵ controls the rate of the circuit dynamics.

In the first setup, we fix the subsystem A and starting from the computational basis state $|\psi_1\rangle = |0\dots 0\rangle$, we monitor the resource monotones (1)–(3) in the reduced state of the subsystem $\rho_A(t) = \text{tr}_{\bar{A}}[|\psi(t)\rangle\langle\psi(t)|]$, where $|\psi(t)\rangle = U_t |\psi_1\rangle$ is the time-evolved state and \bar{A} denotes the complement of A . For suitable gate ensembles, this setup enables us to track how the circuits generate the resources acting on $|\psi_1\rangle$ which is a free state of for theories of nonstabilizerness, coherence and non-Gaussianity.

In the second setup, the circuit comprises gates that are free operations, while the resource is localized in a finite “cluster” of the initial state $|\psi_2\rangle$, taken of the form $|\psi_2\rangle = |0\dots 0\rangle \otimes |m\rangle \otimes |0\dots 0\rangle$, where $|m\rangle$ denotes a resourceful state localized on L_M central sites of the chain. This setup enables us, by varying the position of the subsystem A , to track how the resources spread throughout the chain under the dynamics of the circuits.

Local resource growth and decay.— Now, we study the first setup by fixing the initial state as $|\psi_1\rangle$ and monitoring the resource content of the subsystem state ρ_A .

Nonstabilizerness. To track the dynamics of LRoM, (1), we choose the gates $u_{i,j}$ in (4) as Haar-random unitaries from the unitary group $\mathcal{U}(4)$. Fixing the system size to $L = 24$ and considering $L_A \leq 4$, we perform full statevector simulation to compute $\rho_A(t)$ and then we evaluate $\mathcal{L}(\rho_A(t))$ [111]. The results are shown in Fig. 2(a). The gates generate nonstabilizerness and $\mathcal{L}(\rho_A)$ grows, reaching a maximum at time $\tau_{\mathcal{L}}^m$. This maximum occurs at a time $\tau_{\mathcal{L}}^m \sim \log L_A$, as shown in the bottom inset of Fig. 2(a). The logarithmic scaling of

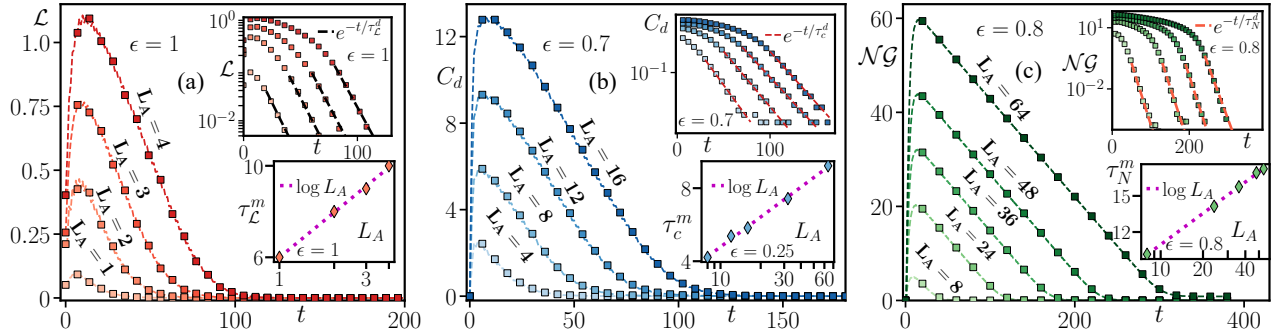


Figure 2. Local dynamics of (a) LRoM $\mathcal{L}(\rho_A)$ ($L = 24$), (b) relative entropy of coherence $C_d(\rho_A)$ ($L = 128$), and (c) relative entropy of non-Gaussianity $\mathcal{NG}(\rho_A)$ ($L = 128$) for subsystems of size L_A under resource-generating circuits initialized in the free state $|\Psi_1\rangle$. Results are averaged over at least 10^4 circuit realizations; the dilution parameter ϵ in each panel is chosen for clarity. Main panels: the rise-peak-fall structure of resource content of $\rho_A(t)$. Top insets: exponential relaxation of the monotones at large t . Bottom insets: peak times scale logarithmically with subsystem size, $\tau^m \sim \log L_A$.

τ_L^m is reminiscent of the logarithmic-in-system-size saturation of global nonstabilizerness measures under random circuit dynamics [85]. At later times, the dynamics strongly entangles subsystem A with its complement \bar{A} , and ρ_A gradually approaches the maximally mixed state, $\rho_A \xrightarrow{t \gg 1} \mathbb{1}_A/2^{L_A}$, where $\mathbb{1}_A$ is the identity operator on A . The maximally mixed state belongs to STAB, and LRoM decays exponentially to 0, $\mathcal{L}(\rho_A(t)) \propto e^{-t/\tau_L^d}$, with a decay time τ_L^d independent of the subsystem size; $\mathcal{L}(\rho_A(t))$ reaches a fixed threshold $\theta \ll 1$ on a timescale proportional to L_A , see [118] for further analysis.

Coherence and non-Gaussianity. The characteristic rise-peak-fall structure of the local resource content under local random circuit dynamics is also found for the measures of coherence (2) and fermionic non-Gaussianity (3), as we demonstrate in the following. To obtain a clearer picture of the local resource dynamics, we restrict the gates $u_{i,j}$ in (4) to be Clifford gates, which enables numerical simulations of systems comprising hundreds of qubits via the tableaux formalism [119], far beyond the reach of full statevector simulations.

To study the relative entropy of coherence of ρ_A , we choose the gates $u_{i,j}$ from the subset $C_2 \setminus C_2^{\text{inc}}$ of the 11520 two-qubit Clifford gates C_2 , where C_2^{inc} denotes the set of 768 *incoherent* Clifford unitaries that do not generate coherence (superpositions of two or more computational-basis states) when acting on computational-basis states. Using numerical simulations [120] of a chain of $L = 128$ qubits and computing $C_d(\rho_A)$ within the tableaux formalism via the formula derived in [102], we obtain the results shown in Fig. 2(b). As in the case of nonstabilizerness, we observe a rise-peak-fall structure of $C_d(\rho_A(t))$, with a peak at times $\tau_c^m \propto \log L_A$, reminiscent of the log-depth anticoncentration [3, 79], now visible over a considerably wider range of subsystem sizes $L_A \leq 64$, and an exponential decay $C_d(\rho_A(t)) \propto e^{-t/\tau_c^d}$ for $t \gg 1$. The dynamics saturates

down to a fixed threshold $\theta \ll 1$ on timescales scaling linearly with L_A , see also [118].

Clifford gates C_2 contain a subset of 192 Clifford matchgates C_2^{Gauss} , which are Clifford unitaries that also fulfill the matchgate condition [121–123], i.e., they are fermionic Gaussian unitaries. To study the evolution of $\mathcal{NG}(\rho_A(t))$, we choose the gates $u_{i,j}$ in (4) randomly from the set $C_2 \setminus C_2^{\text{Gauss}}$, and simulate a chain of $L = 128$ qubits within the tableaux formalism [120]. The results shown in Fig. 2(c) again exhibit a rise-peak-fall structure, with the peak time $\tau_N^m \propto \log L_A$, consistently with the similarity of fermionic magic resources growth [34] to dynamics of coherence and nonstabilizerness, and an exponential decay $\mathcal{NG}(\rho_A(t)) \propto e^{-t/\tau_N^d}$ at long times.

Resource spreading.— We now turn to the second setup, where the system is initialized in a locally resourceful state $|\psi_2\rangle$ and the gates $u_{i,j}$ are chosen as free operations of the respective resource theory.

Nonstabilizerness. To study the spreading of nonstabilizerness, we draw each gate $u_{i,j}$ uniformly from the set C_2 of two-qubit Clifford gates, and prepare the initial state $|\psi_2\rangle = |0\dots 0\rangle \otimes |m\rangle \otimes |0\dots 0\rangle$, with $|m\rangle = |T\rangle^{\otimes L_M}$ a product of single-qubit magic states $|T\rangle = \cos(\pi/8)|0\rangle + \sin(\pi/8)|1\rangle$ [124]. We fix $L_M = 4$, perform statevector simulations for $L = 24$ qubits to obtain the time-evolved state $|\psi(t)\rangle = U_t|\psi_2\rangle$, and compute $\mathcal{L}(\rho_A(t))$. We introduce a variable $x_r \in [-L/2, L/2]$ denoting the relative position of the center-of-mass of subsystem A respective to the center of the magic region. The resulting spatiotemporal profile of $\mathcal{L}(\rho_A)$ is shown in Fig. 3(1a).

The spacetime profile of nonstabilizerness exhibits a clear light-cone structure, signaling ballistic spreading of the resource. The earliest detectable nonstabilizerness time grows linearly with the distance x_r of subsystem A from the initial magic cluster, defining an outer light cone expanding with velocity $v_{\mathcal{L}b} = 1$ set by gate locality. Along this front, $\mathcal{L}(\rho_A)$ decays exponentially with distance and at larger distances (e.g. $x_r = 8$ and $t = 8$),

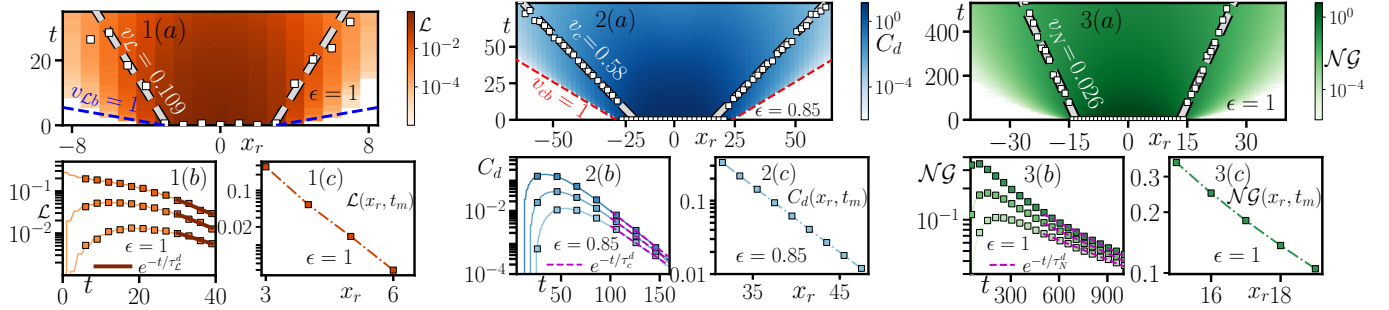


Figure 3. Spreading of (1) nonstabilizerness ($L = 24$), (2) coherence ($L = 256$), and (3) non-Gaussianity ($L = 128$) from a localized resource cluster under circuits comprising resource-free gates. The results are averaged over 10^4 circuit realizations. Panels (a) display the emergence of ballistic light cone structure of the spreading; panels (b) show the evolution of the resource content of ρ_A at fixed x_r ($-x_r = (5, 4, 3), (47.5, 41.5, 35.5)$ and $(19, 17, 15)$ for $R = \mathcal{L}, c, N$, respectively.); panels (c) highlight the exponential attenuation of the peak local resource with distance along the light cone $x = v_{Rt} + \text{const}$ (with $R = \mathcal{L}, c, N$).

it falls below the threshold 10^{-6} . After the first nonzero signal at fixed x_r , the nonstabilizerness of ρ_A increases, see Fig. 3(1b), reaching a maximum at times t_m satisfying $x_r = v_{\mathcal{L}} t_m + \text{const}$, which reflects ballistic spreading of nonstabilizerness. The peak LRoM decays exponentially with x_r [Fig. 3(1c)]. At late times, $\mathcal{L}(\rho_A)$ decays exponentially back to zero [Fig. 3(1b)] as ρ_A approaches the maximally mixed state. This return of every small subsystem to a free state at long times shows that magic is not a conserved local density under free two-body dynamics: the initially localized resource is transferred into highly nonlocal correlations, so that local magic quantified by $\mathcal{L}(\rho_A)$ vanishes even though global nonstabilizerness measures of $|\psi(t)\rangle$ remain constant at all t , since U_t consists of stabilizer operations.

Coherence and non-Gaussianity. We restrict the gates $u_{i,j}$ to Clifford unitaries [119, 120] to study the spreading of coherence and fermionic non-Gaussianity in chains comprising hundreds of qubits.

For coherence, we choose each $u_{i,j}$ to be the SWAP gate with probability p , and with probability $1 - p$ a randomly chosen gate from the set C_2^{inc} . The initial state is prepared as $|\psi_2\rangle = |0\dots0\rangle \otimes |m\rangle \otimes |0\dots0\rangle$, with $|m\rangle = [(|0\rangle + |1\rangle)/\sqrt{2}]^{\otimes L_c}$ acting as a source of coherence. Fixing $L = 256$, $L_c = 32$ and $L_A = 32$, we compute the relative entropy of coherence $C_d(\rho_A)$ as a function of time t and the position x_r of subsystem A. Our results, shown in Fig. 3(2a)–(2c), uncover a spatiotemporal pattern of $C_d(\rho_A)$ analogous to the nonstabilizerness case, with light cones at velocity $v_{cb} = 1$ delimiting the region of nonzero coherence and a maximum of $C_d(\rho_A)$ propagating along a light cone with velocity $v_c < 1$.

For non-Gaussianity, we choose the gates $u_{i,j}$ in (4) randomly from the Clifford matchgate set C_2^{Gauss} , while the initial state is $|\psi_2\rangle = |0\dots0\rangle \otimes |m\rangle \otimes |0\dots0\rangle$, with $|m\rangle = [\frac{1}{4}(|0000\rangle + |1100\rangle + |0011\rangle - |1111\rangle)]^{\otimes L_N}$ a product of four-qubit fermionic magic states [125]. Setting $L = 128$,

$L_N = 4$, and $L_A = 16$, we obtain the results for $\mathcal{NG}(\rho_A)$ shown in Fig. 3(3a)–(3c), which reveal a spatiotemporal structure of non-Gaussianity spreading fully analogous to the nonstabilizerness and coherence cases.

Discussion.— The rise-peak-fall structure of the local resource content summarized in Fig. 2 stems from a competition between resource injection by resource-generating gates, which increases the local resource, and the buildup of entanglement and long-range correlations at later times, which drive ρ_A towards the maximally mixed state and suppress the resource measures. A similar behavior was observed [126] for entanglement flatness [127], which bounds nonlocal nonstabilizerness [128]. The ballistic spreading of resources in Fig. 3 arises from the generation of nonlocal correlations across the chain by the circuit dynamics, which simultaneously causes an exponential attenuation of the local resource content, sharply distinguishing resource spreading from the transport of conserved local densities. To corroborate the generality of our findings, we show in the End Matter that the same phenomenology governs the spatiotemporal dynamics of mana, a nonstabilizerness monotone [19], in qutrit chains evolved under local circuits. We further show that coherence spreading in non-Clifford circuits exhibits the same behavior, using large-scale simulations whose cost scales exponentially only in the size of the coherent cluster L_c and polynomially in the total system size L , analogous to simulation methods for Clifford circuits doped with nonstabilizer gates [129, 130].

Conclusions.— In this work, we studied the spreading of quantum resources that underlie the classical complexity of quantum states: nonstabilizerness, coherence, and fermionic non-Gaussianity, in local random circuit dynamics. For resource-generating gates, we uncovered a rise–peak–decay behavior of the local resource content, with peak times scaling logarithmically with the subsystem size, $\tau^m \sim \log L_A$. This signals a rapid onset of local

resourcefulness and the buildup of nonclassical features in local subsystems on a timescale parametrically shorter than the linear timescale required to generate correlations across the subsystem. In a complementary setup, where the gates are free operations that do not generate the resource and the chain is initialized with a localized resourceful cluster, we found ballistic spreading of the local resource content. Taken together, our results demonstrate a unified phenomenology for the spatiotemporal dynamics of nonstabilizerness, coherence, and fermionic non-Gaussianity, pointing to a form of universality in resource spreading governed primarily by locality and unitarity, rather than microscopic details of the dynamics or of the specific resource theory. We therefore conjecture that the phenomenology uncovered here applies broadly to local ergodic quantum many-body systems.

Our results open several conceptual avenues for exploration. A central challenge is to develop an analytical framework for the phenomenology uncovered here, for instance by relating nonstabilizerness and related resources to the slow hydrodynamic modes [77, 131–133] of many-body dynamics or utilizing the replica trick to perform calculations, a first step in that direction in the limit of infinite local Hilbert space dimension was already done in [134]. It would also be compelling to move beyond random circuits to fully ergodic Floquet drives [86, 135] and genuinely chaotic Hamiltonian evolutions [136], where similar universal structures may emerge in a less coarse-grained setting. Moreover, incorporating symmetries [86] and probing the role of integrability [137] and ergodicity breaking [46, 47, 138–140] could shed further light on more exotic regimes of quantum resource spreading. We leave these questions for future work.

Acknowledgments.— This work is dedicated to Ada. We thank Diptiman Sen and Sumilan Banerjee for comments and suggestions, and Emanuele Tirrito for insightful discussions and collaboration on related projects. S.A. acknowledges support from the Alexander von Humboldt Foundation as a Humboldt postdoctoral fellow. X.T. acknowledges support from DFG under Germany’s Excellence Strategy – Cluster of Excellence Matter and Light for Quantum Computing (ML4Q) EXC 2004/1 – 390534769, and DFG Collaborative Research Center (CRC) 183 Project No. 277101999 - project B01. P.S. acknowledges fellowship within the “Generación D” initiative, Red.es, Ministerio para la Transformación Digital y de la Función Pública, for talent attraction (C005/24-ED CV1), funded by the European Union NextGenerationEU funds, through PRTR.

Note Added: While completing this manuscript, we became aware of two independent studies by Maity, Hamazaki [141], and Bejan, Claeys, Yao [142] on the spreading of local magic under Clifford dynamics. While approach of our study is markedly different, the results agree in the overlapping regime.

End matter

Local mana spreading in qutrits.— We further substantiate the picture of nonstabilizerness spreading established for qubits in the main text by examining local resource dynamics in a one-dimensional chain of L qutrits (onsite Hilbert space dimension $d = 3$). As a probe of the resource content in a subsystem A , we employ the mana [19], a Wigner-function-based quantifier of nonstabilizerness that constitutes a faithful magic monotone for mixed states. Let $\omega = e^{2\pi i/d}$ and introduce the generalized Pauli operators

$$Z = \sum_{m=0}^{d-1} \omega^m |m\rangle\langle m|, \quad X = \sum_{m=0}^{d-1} |m+1 \bmod d\rangle\langle m|. \quad (5)$$

On an L -site chain, we denote by X_ℓ and Z_ℓ the corresponding operators acting on site ℓ . For each phase-space point $r = (r_1^x, r_1^z, \dots, r_L^x, r_L^z) \in \mathbb{Z}_d^{2L}$, we define the Pauli string $P_r = \prod_{\ell=1}^L \omega^{\frac{(d+1)}{2}r_\ell^x r_\ell^z} X_\ell^{r_\ell^x} Z_\ell^{r_\ell^z}$. These operators generate the phase-point operators [143]

$$A_0 = \frac{1}{d^L} \sum_{r \in \mathbb{Z}_d^{2L}} P_r, \quad A_r = P_r A_0 P_r^\dagger, \quad (6)$$

which in turn define the discrete Wigner function

$$W_r(\rho) = \text{tr}(A_r \rho) / d^L. \quad (7)$$

The nonstabilizerness of a state ρ is then quantified by the mana [19, 85, 144, 145]

$$\mathcal{M}(\rho) = \log_2 \left(\sum_{r \in \mathbb{Z}_d^{2L}} |W_r(\rho)| \right), \quad (8)$$

which vanishes for stabilizer states and increases monotonically with the negativity of the Wigner quasi-probability distribution.

With these qutrit degrees of freedom in place, we perform an analysis fully analogous to the qubit case. In the first setup, starting from the resource-free product state $|0\dots0\rangle$ and evolving under local two-qutrit Haar-random gates—we find that the local nonstabilizerness in A displays the same universal rise–peak–fall profile as the one observed for qubits, illustrated in Fig. 4(1a)–(1c) for $L = 16$ and $L_A = 2\text{--}7$. In particular, the timescale τ_M^m at which the reduced mana in A attains its maximum again grows only logarithmically with the subsystem size, $\tau_M^m \propto \log L_A$ [bottom inset of Fig. 4(1c)], thereby reinforcing the fast-scrambling phenomenology of local magic spreading across different on-site Hilbert space dimensions. Furthermore, Fig. 4(2a)–(2c) shows the space–time pattern of local mana in a chain of $L = 14$ qutrits, initialized in a state featuring a magic cluster of size $L_M = 5$ where each single-qutrit magic state being $|m\rangle = e^{-i\frac{2\pi}{9}(X_i+X_i^\dagger)}|0\rangle$ and evolved under a global brick-work circuit composed of random uniformly sampled two-qutrit Clifford gates $u \in C_2(d)$ [146]. The resulting mana

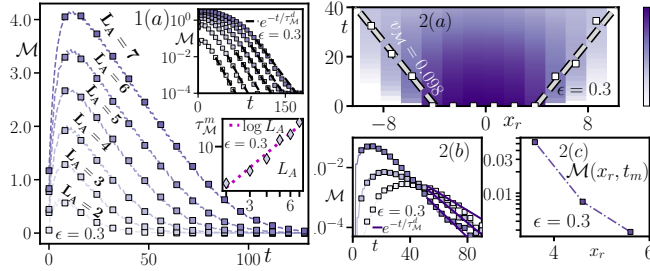


Figure 4. Dynamics of mana $\mathcal{M}(\rho_A)$ in qutrit chains. Panel (1): evolution from a resource-free initial state under resourceful two-qutrit Haar gates for $L = 16$ and various L_A , showing a universal rise-peak-fall profile (main), late-time exponential decay (top inset), and peak times scaling logarithmically with L_A (bottom inset). Panel (2): $\mathcal{M}(\rho_A)$ for $L = 14$ with an initial magical cluster of size $L_M = 5$ and $L_A = 3$ under resource-free gates, exhibiting a light-cone spreading pattern and late-time exponential decay to a free state. Results averaged over at least 10^4 circuit realizations and overall dilution ϵ in each panel are chosen for clarity.

fronts for the subsystem of size $L_A = 3$ closely parallel the nonstabilizerness spreading observed in the qubit case (Fig. 2(1a)–(1c)), indicating that the qualitative features of local magic transport are robust to the underlying on-site dimensionality.

Local coherence spreading using sparse-vector simulation.— To corroborate our findings in the coherence case, we additionally employ sparse-vector simulations, which enable access to system sizes far beyond the reach of the full statevector simulations. The central structural property we exploit is that the coherence-preserving local two-qubit gates are of the form $U_{\pi, \vec{\phi}} = \sum_{b \in \{00, 01, 10, 11\}} e^{i\phi_b} |\pi(b)\rangle\langle b|$, where π is one of the 24 permutations of the two-qubit computational-basis states and $\vec{\phi} \equiv (\phi_b)$ denotes four arbitrary phases, so that the gate merely permutes computational-basis states and decorates them with phases. Consider a one-dimensional qubit chain of length L with an prepared in a state $|\psi_2\rangle = |0\dots 0\rangle \otimes |m\rangle \otimes |0\dots 0\rangle$, where $|m\rangle$ is a superposition of basis states on L_c qubits. The state $|\psi_2\rangle$ is supported on exactly $N_+(0) = 2^{L_c}$ computational-basis configurations out of the full Hilbert space of dimension 2^L . Because the global time-evolution operator is built as a product of two-qubit gates that only permute the local states and add phases, the number of nonzero amplitudes is conserved at all times, $N_+(t) = N_+(0) = 2^{L_c}$ for every circuit layer t . This conservation of sparsity of the statevector is what renders the sparse-vector simulation efficient even for large L : although the underlying Hilbert space is exponentially large, the dynamics is confined to a smaller subspace of size $2^{L_c} \ll 2^L$, and it suffices to keep track of only 2^{L_c} nonzero amplitudes to compute the state of the system at any circuit depth t . This yields a computational cost scaling exponentially

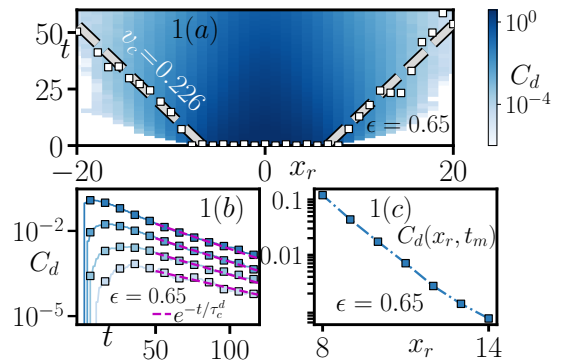


Figure 5. Coherence spreading for a chain of $L = 64$ qubits from initially localized resource cluster, evolved under random coherence preserving gates and computed via sparse-vector simulations, with $L_c = 0$ and $L_A = 8$. Panel (a) reveals a clear two-front structure in the dynamics, with a sharply defined inner light cone. Panel (b-c) illustrates the late-time relaxation of the local resource content back to a resource-free steady state and exponential attenuation of the peak local resource with distance from the initial cluster.

with L_c but only polynomially with system size L , similarly to the approach of [129, 130] to Clifford circuits doped with beyond Clifford gates.

In our numerical simulations, we investigate a chain of total size $L = 64$ with an initial magic cluster of size $L_c = 8$ prepared in $|+\rangle$ states and embedded in a background of resource-free states $|0\rangle$, such that $N_+(t) = 2^{L_c} = 256$ for all t . The dynamics is generated by the coherence-preserving two-qubit gates specified above, the relative entropy of coherence $C_d(\rho_A)$ is evaluated for a subsystem of size $L_A = 8$, the overall gate dilution is fixed at $\epsilon = 0.65$, and all observables are averaged over 10^4 random circuit realizations. Within this approach, we obtain results shown in Fig. 5 finding behavior that is quantitatively similar to the Clifford case analyzed in Fig. 3(2a)-(2c). In particular, we observe a clear ballistic spreading of the local resource content $C_d(\rho_A)$ and an exponential suppression of $C_d(\rho_A)$ at larger times and distances.

Ballistic propagation of outer front in the non-Gaussianity spreading.— In Fig. 3, we observed that the spatiotemporal region of nonzero nonstabilizerness and coherence is delimited by a light cone corresponding velocity $v_{\mathcal{L}b} = 1 = v_{cb}$. In contrast, a light cone delimiting the region of non-vanishing $\mathcal{NG}(\rho_A)$ corresponds to a smaller velocity. To elucidate this behavior, we uncover a directional structure within the set of Clifford matchgates: there exist two distinguished classes matchgates, one transporting the resource of non-Gaussianity ballistically to the left and the other ballistically to the right. Crucially, no single matchgate generates simultaneous left- and right-moving ballistic propagation. Moreover, the associated ballistic velocity is comparatively

smaller, resulting in non-Gaussianity spreading still ballistically, but slower than the coherence and nonstabilizerness. In addition, the resource content in reduced subsystems away from the magic center decays exponentially with distance, further suppressing long-range non-Gaussian correlations. Taken together, these effects explain why a sharp ballistic outer front is not readily visible for the non-Gaussianity spreading.

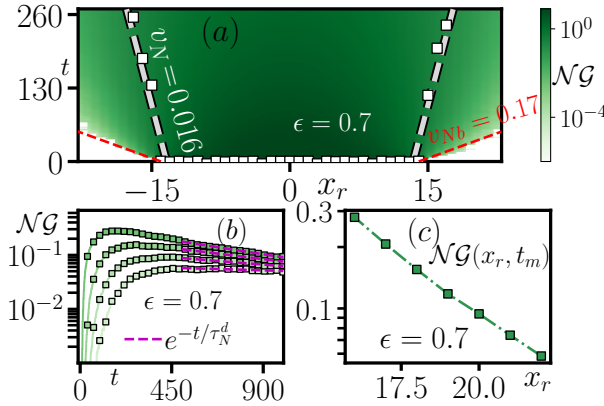


Figure 6. Spatiotemporal spreading of a localized non-Gaussian magic cluster in a 128-qubit chain under resource-free two-body Gaussian (matchgate) dynamics, selecting $u_{i,j}$ gates from 10 Clifford matchgates propagating the initial non-Gaussian cluster in left- and right-moving ballistic modes and 10 generic Clifford matchgates. We fix $(L_M, L_A) = (16, 16)$, set $\epsilon = 0.7$, and average over 10^4 circuit realizations. The outer front in panel (a) is markedly more visible than in the case of Fig. 3(c), highlighting the role of the left/right propagating gates; all other features in panels (a–c) remain qualitatively the same as in Fig. 3.

To sharpen this picture, we perform numerical simulations in which we explicitly include both the left- and right-moving Clifford matchgates, supplemented by an additional set of ten generic matchgates, for a chain of length $L = 128$ and averaging the results over at least 10^4 circuit realizations. In this tailored setting, the ballistic propagation of the region of nonzero $\mathcal{N}\mathcal{G}(\rho_A)$ becomes strikingly more pronounced than in the fully generic matchgate ensemble, as shown in panel (a) in Fig. 6. Other features of spatiotemporal resource propagation remain qualitatively the same as shown in Fig. 3 (c).

tanglement in many-body systems, *Reviews of Modern Physics* **80**, 517 (2008).

- [3] A. M. Dalzell, N. Hunter-Jones, and F. G. S. L. Brandão, Random quantum circuits anticoncentrate in log depth, *PRX Quantum* **3**, 010333 (2022).
- [4] P. Sierant and X. Turkeshi, Universal behavior beyond multifractality of wave functions at measurement-induced phase transitions, *Phys. Rev. Lett.* **128**, 130605 (2022).
- [5] P. W. Claeys and G. De Tomasi, Fock-space delocalization and the emergence of the porter-thomas distribution from dual-unitary dynamics, *Phys. Rev. Lett.* **134**, 050405 (2025).
- [6] B. Magni and X. Turkeshi, Quantum complexity and chaos in many-qudit doped clifford circuits, arXiv preprint 10.48550/arXiv.2506.02127 (2025), arXiv:2506.02127 [quant-ph].
- [7] A. Sauliere, B. Magni, G. Lami, X. Turkeshi, and J. De Nardis, Universality in the anticoncentration of chaotic quantum circuits, *Phys. Rev. B* **112**, 134312 (2025).
- [8] A. Bouland, B. Fefferman, C. Nirkhe, and U. Vazirani, On the complexity and verification of quantum random circuit sampling, *Nature Physics* **15**, 159–163 (2018).
- [9] G. Lami, J. De Nardis, and X. Turkeshi, Anticoncentration and state design of random tensor networks, *Phys. Rev. Lett.* **134**, 010401 (2025).
- [10] M. Fava, J. Kurchan, and S. Pappalardi, Designs via free probability, *Phys. Rev. X* **15**, 011031 (2025).
- [11] Z. Cheng, X. Feng, and M. Ippoliti, Pseudoentanglement from tensor networks, *Phys. Rev. Lett.* **135**, 020403 (2025).
- [12] M. Ippoliti and W. W. Ho, Dynamical purification and the emergence of quantum state designs from the projected ensemble, *PRX Quantum* **4**, 030322 (2023).
- [13] P. W. Claeys and A. Lamacraft, Emergent quantum state designs and biunitarity in dual-unitary circuit dynamics, *Quantum* **6**, 738 (2022).
- [14] T. Schuster, J. Haferkamp, and H.-Y. Huang, Random unitaries in extremely low depth, *Science* **389**, 92–96 (2025).
- [15] R. P. Feynman, Simulating physics with computers, *International Journal of Theoretical Physics* **21**, 467 (1982).
- [16] J. I. Cirac and P. Zoller, Goals and opportunities in quantum simulation, *Nature Physics* **8**, 264 (2012).
- [17] K. Bharti, A. Cervera-Lierta, T. H. Kyaw, T. Haug, S. Alperin-Lea, A. Anand, M. Degroote, H. Heimonen, J. S. Kottmann, T. Menke, W.-K. Mok, S. Sim, L.-C. Kwek, and A. Aspuru-Guzik, Noisy intermediate-scale quantum algorithms, *Rev. Mod. Phys.* **94**, 015004 (2022).
- [18] E. Chitambar and G. Gour, Quantum resource theories, *Rev. Mod. Phys.* **91**, 025001 (2019).
- [19] V. Veitch, S. A. Hamed Mousavian, D. Gottesman, and J. Emerson, The resource theory of stabilizer quantum computation, *New Journal of Physics* **16**, 013009 (2014).
- [20] Z.-W. Liu and A. Winter, Many-body quantum magic, *PRX Quantum* **3**, 020333 (2022).
- [21] L. Leone, S. F. E. Oliviero, and A. Hamma, Stabilizer rényi entropy, *Phys. Rev. Lett.* **128**, 050402 (2022).
- [22] S. Bravyi, G. Smith, and J. Smolin, Trading classical and quantum computational resources, *Phys. Rev. X* **6**, 021043 (2016).

* asreemay@uni-koeln.de

† xturkesh@uni-koeln.de

‡ piotr.sierant@bsc.es

- [1] R. Horodecki, P. Horodecki, M. Horodecki, and K. Horodecki, Quantum entanglement, *Reviews of Modern Physics* **81**, 865 (2009).
- [2] L. Amico, R. Fazio, A. Osterloh, and V. Vedral, En-

- [23] X. Wang, M. M. Wilde, and Y. Su, Quantifying the magic of quantum channels, *New Journal of Physics* **21**, 103002 (2019).
- [24] M. Howard and E. T. Campbell, Application of a resource theory for magic states to fault-tolerant quantum computing, *Phys. Rev. Lett.* **118**, 090501 (2017).
- [25] T. Baumgratz, M. Cramer, and M. B. Plenio, Quantifying coherence, *Phys. Rev. Lett.* **113**, 140401 (2014).
- [26] A. Streltsov, G. Adesso, and M. B. Plenio, Colloquium: Quantum coherence as a resource, *Reviews of Modern Physics* **89**, 041003 (2017).
- [27] G. Saxena, Dynamical resource theory of quantum coherence, *Phys. Rev. Res.* **2**, 023298 (2020).
- [28] Q. Zhuang, Resource theory of non-gaussian operations, *Phys. Rev. A* **97**, 052317 (2018).
- [29] R. Takagi, Convex resource theory of non-gaussianity, *Phys. Rev. A* **97**, 062337 (2018).
- [30] M. Hebenstreit, R. Jozsa, B. Kraus, S. Strelchuk, and M. Yoganathan, All pure fermionic non-gaussian states are magic states for matchgate computations, *Phys. Rev. Lett.* **123**, 080503 (2019).
- [31] L. Lumia, E. Tirrito, R. Fazio, and M. Collura, Measurement-induced transitions beyond gaussianity: A single particle description, *Phys. Rev. Res.* **6**, 023176 (2024).
- [32] X. Lyu and K. Bu, Fermionic gaussian testing and non-gaussian measures via convolution (2024), arXiv:2409.08180 [quant-ph].
- [33] L. Coffman, G. Smith, and X. Gao, Measuring non-gaussian magic in fermions: Convolution, entropy, and the violation of wick's theorem and the matchgate identity (2025), arXiv:2501.06179 [quant-ph].
- [34] P. Sierant, P. Stornati, and X. Turkeshi, Fermionic magic resources of quantum many-body systems (2025), arXiv:2506.00116 [quant-ph].
- [35] F. Haake, *Quantum Signatures of Chaos* (Springer, Berlin, 2010).
- [36] A. M. Läuchli and C. Kollath, Spreading of correlations and entanglement after a quench in the one-dimensional bose–hubbard model, *Journal of Statistical Mechanics: Theory and Experiment* **2008**, P05018 (2008).
- [37] H. Kim and D. A. Huse, Ballistic spreading of entanglement in a diffusive nonintegrable system, *Phys. Rev. Lett.* **111**, 127205 (2013).
- [38] R. J. Garcia, K. Bu, and A. Jaffe, Resource theory of quantum scrambling, *Proceedings of the National Academy of Sciences* **120**, e2217031120 (2023), <https://www.pnas.org/doi/pdf/10.1073/pnas.2217031120>.
- [39] B. Swingle, G. Bentsen, M. Schleier-Smith, and P. Hayden, Measuring the scrambling of quantum information, *Phys. Rev. A* **94**, 040302 (2016).
- [40] N. Yunger Halpern, A. Bartolotta, and J. Pollack, Entropic uncertainty relations for quantum information scrambling, *Communications Physics* **2**, 92 (2019).
- [41] A. Vikram, L. Shou, and V. Galitski, Proof of a universal speed limit on fast scrambling in quantum systems (2024), arXiv:2404.15403 [quant-ph].
- [42] M. Kaneyasu and Y. Hasegawa, Unified quantification of entanglement and magic in information scrambling and their trade-off relationship (2025), arXiv:2508.11969 [quant-ph].
- [43] J. Odavić, M. Viscardi, and A. Hamma, Stabilizer entropy in nonintegrable quantum evolutions, *Phys. Rev. B* **112**, 104301 (2025).
- [44] L. D'Alessio, Y. Kafri, A. Polkovnikov, and M. Rigol, From quantum chaos and eigenstate thermalization to statistical mechanics and thermodynamics, *Advances in Physics* **65**, 239–362 (2016).
- [45] S. Pappalardi, L. Foini, and J. Kurchan, Eigenstate thermalization hypothesis and free probability, *Physical Review Letters* **129**, 170603 (2022).
- [46] D. A. Abanin, E. Altman, I. Bloch, and M. Serbyn, Colloquium: Many-body localization, thermalization, and entanglement, *Reviews of Modern Physics* **91**, 021001 (2019).
- [47] P. Sierant, M. Lewenstein, A. Scardicchio, L. Vidmar, and J. Zakrzewski, Many-body localization in the age of classical computing, *Reports on Progress in Physics* **88**, 026502 (2025).
- [48] E. Tirrito, P. S. Tarabunga, D. S. Bhakuni, M. Dalmonte, P. Sierant, and X. Turkeshi, *Universal spreading of nonstabilizerness and quantum transport* (2025), arXiv:2506.12133 [quant-ph].
- [49] B. Jasser, J. Odavić, and A. Hamma, Stabilizer entropy and entanglement complexity in the sachdev-ye-kitaev model, *Phys. Rev. B* **112**, 174204 (2025).
- [50] S. Bera and M. Schirò, *Non-stabilizerness of sachdev-ye-kitaev model* (2025), arXiv:2502.01582 [quant-ph].
- [51] D. Sticlet, B. Dóra, D. Szombathy, G. Zaránd, and C. P. Moca, Nonstabilizerness in open xxz spin chains: Universal scaling and dynamics, *Phys. Rev. Res.* **7**, 043130 (2025).
- [52] P. R. N. Falcão, P. Sierant, J. Zakrzewski, and E. Tirrito, Nonstabilizerness dynamics in many-body localized systems, *Phys. Rev. Lett.* **135**, 240404 (2025).
- [53] T. Haug and L. Piroli, Quantifying nonstabilizerness of matrix product states, *Phys. Rev. B* **107**, 035148 (2023).
- [54] P. S. Tarabunga, E. Tirrito, T. Chanda, and M. Dalmonte, Many-body magic via pauli-markov chains – from criticality to gauge theories, *PRX Quantum* **4**, 040317 (2023), arXiv:2305.18541 [quant-ph].
- [55] P. S. Tarabunga and C. Castelnovo, Magic in generalized rokhsar-kivelson wavefunctions, *Quantum* **8**, 1347 (2024).
- [56] M. Collura, J. D. Nardis, V. Alba, and G. Lami, The non-stabilizerness of fermionic Gaussian states, arXiv preprint 10.48550/arXiv.2412.05367 (2024), arXiv:2412.05367 [quant-ph].
- [57] G. C. Santra, J. Mildenberger, E. Ballini, A. Bottarelli, M. M. Wauters, and P. Hauke, Quantum resources in non-abelian lattice gauge theories: Nonstabilizerness, multipartite entanglement, and fermionic non-gaussianity, arXiv preprint 10.48550/arXiv.2510.07385 (2025), arXiv:2510.07385 [quant-ph].
- [58] C. D. White, C. Cao, and B. Swingle, Conformal field theories are magical, *Physical Review B* **103**, 075145 (2021), arXiv:2007.01303 [quant-ph].
- [59] M. Frau, P. S. Tarabunga, M. Collura, E. Tirrito, and M. Dalmonte, Stabilizer disentangling of conformal field theories, *SciPost Physics* **18**, 165 (2025).
- [60] M. Hoshino, M. Oshikawa, and Y. Ashida, Stabilizer rényi entropy and conformal field theory (2025), arXiv:2503.13599 [quant-ph].
- [61] M. Bejan, C. McLauchlan, and B. Béri, Dynamical magic transitions in monitored clifford+*t* circuits, *PRX Quantum* **5**, 030332 (2024), arXiv:2312.00132 [quant-ph].
- [62] G. E. Fux, E. Tirrito, M. Dalmonte, and R. Fazio,

- Entanglement–nonstabilizerness separation in hybrid quantum circuits, *Physical Review Research* **6**, L042030 (2024), arXiv:2312.02039 [quant-ph].
- [63] E. Tirrito, L. Lumia, A. Paviglianiti, G. Lami, A. Silva, X. Turkeshi, and M. Collura, Magic phase transitions in monitored gaussian fermions, arXiv preprint 10.48550/arXiv.2507.07179 (2025), arXiv:2507.07179 [quant-ph].
- [64] F. B. Trigueros and J. A. M. Guzmán, Nonstabilizerness and error resilience in noisy quantum circuits, arXiv preprint 10.48550/arXiv.2506.18976 (2025), arXiv:2506.18976 [quant-ph].
- [65] T. Hernández-Yanes, P. Sierant, J. Zakrzewski, and M. Płodzień, Non-stabilizerness in quantum-enhanced metrological protocols (2025), arXiv:2510.01380 [quant-ph].
- [66] B. Coecke, T. Fritz, and R. W. Spekkens, A mathematical theory of resources, *Information and Computation* **250**, 59 (2016).
- [67] M. P. A. Fisher, V. Khemani, A. Nahum, and S. Vijay, Random quantum circuits, *Annual Review of Condensed Matter Physics* **14**, 335 (2023).
- [68] A. Nahum, S. Vijay, and J. Haah, Operator spreading in random unitary circuits, *Physical Review X* **8**, 021014 (2018).
- [69] A. Chan, A. D. Luca, and J. T. Chalker, Solution of a minimal model for many-body quantum chaos, *Physical Review X* **8**, 041019 (2018).
- [70] S. Shivam, A. D. Luca, D. A. Huse, and A. Chan, Many-body quantum chaos and emergence of ginibre ensemble, *Physical Review Letters* **130**, 140403 (2023).
- [71] A. Nahum, J. Ruhman, S. Vijay, and J. Haah, Quantum entanglement growth under random unitary dynamics, *Physical Review X* **7**, 031016 (2017).
- [72] T. Zhou and A. Nahum, Emergent statistical mechanics of entanglement in random unitary circuits, *Physical Review B* **99**, 174205 (2019).
- [73] R. Vasseur, A. C. Potter, Y.-Z. You, and A. W. W. Ludwig, Entanglement transitions from holographic random tensor networks, *Physical Review B* **100**, 134203 (2019).
- [74] P. Sierant, M. Schirò, M. Lewenstein, and X. Turkeshi, Entanglement growth and minimal membranes in $(d+1)$ random unitary circuits, *Physical Review Letters* **131**, 230403 (2023).
- [75] T. Zhou and A. Nahum, Entanglement membrane in chaotic many-body systems, *Physical Review X* **10**, 031066 (2020).
- [76] G. M. Sommers, S. Gopalakrishnan, M. J. Gullans, and D. A. Huse, Zero-temperature entanglement membranes in quantum circuits, *Physical Review B* **110**, 064311 (2024).
- [77] C. W. von Keyserlingk, T. Rakovszky, F. Pollmann, and S. L. Sondhi, Operator hydrodynamics, otocs, and entanglement growth in systems without conservation laws, *Physical Review X* **8**, 021013 (2018), arXiv:1705.08910 [cond-mat.stat-mech].
- [78] C. Bertoni, J. Haferkamp, M. Hinsche, M. Ioannou, J. Eisert, and H. Pashayan, Shallow shadows: Expectation estimation using low-depth random clifford circuits, *Physical Review Letters* **133**, 020602 (2024).
- [79] X. Turkeshi and P. Sierant, Hilbert space delocalization under random unitary circuits, *Entropy* **26**, 471 (2024).
- [80] D. García-Martín, P. Braccia, and M. Cerezo, Architectures and random properties of symplectic quantum circuits, arXiv preprint 10.48550/arXiv.2405.10264 (2024), arXiv:2405.10264 [quant-ph].
- [81] P. Braccia, P. Bermejo, L. Cincio, and M. Cerezo, Computing exact moments of local random quantum circuits via tensor networks, *Quantum Machine Intelligence* **6**, 54 (2024).
- [82] A. Christopoulos, A. Chan, and A. D. Luca, Universal distributions of overlaps from generic dynamics in quantum many-body systems, *Physical Review Research* **7**, 043035 (2025).
- [83] B. Magni, A. Christopoulos, A. D. Luca, and X. Turkeshi, Anticoncentration in clifford circuits and beyond: From random tensor networks to pseudomagic states, *Physical Review X* **15**, 031071 (2025).
- [84] Y. Zhang, S. Vijay, Y. Gu, and Y. Bao, Designs from magic-augmented clifford circuits, arXiv preprint 10.48550/arXiv.2507.02828 (2025), arXiv:2507.02828 [quant-ph].
- [85] X. Turkeshi, E. Tirrito, and P. Sierant, Magic spreading in random quantum circuits, *Nature Communications* **16**, 2575 (2025).
- [86] E. Tirrito, X. Turkeshi, and P. Sierant, Anticoncentration and nonstabilizerness spreading under ergodic quantum dynamics, *Physical Review Letters* **135**, 220401 (2025).
- [87] A. De Luca and A. Scardicchio, Ergodicity breaking in a model showing many-body localization, *EPL (Europhysics Letters)* **101**, 37003 (2013).
- [88] N. Macé, F. Alet, and N. Laflorencie, Multifractal scalings across the many-body localization transition, *Phys. Rev. Lett.* **123**, 180601 (2019).
- [89] J.-M. Stéphan, S. Furukawa, G. Misguich, and V. Pasquier, Shannon and entanglement entropies of one- and two-dimensional critical wave functions, *Phys. Rev. B* **80**, 184421 (2009).
- [90] J.-M. Stéphan, G. Misguich, and V. Pasquier, Rényi entropy of a line in two-dimensional ising models, *Phys. Rev. B* **82**, 125455 (2010).
- [91] D. J. Luitz, F. Alet, and N. Laflorencie, Universal behavior beyond multifractality in quantum many-body systems, *Phys. Rev. Lett.* **112**, 057203 (2014).
- [92] D. J. Luitz, X. Plat, N. Laflorencie, and F. Alet, Improving entanglement and thermodynamic rényi entropy measurements in quantum monte carlo, *Phys. Rev. B* **90**, 125105 (2014).
- [93] Y. Y. Atas and E. Bogomolny, Multifractality of eigenfunctions in spin chains, *Phys. Rev. E* **86**, 021104 (2012).
- [94] J. Lindinger, A. Buchleitner, and A. Rodríguez, Many-body multifractality throughout bosonic superfluid and mott insulator phases, *Phys. Rev. Lett.* **122**, 106603 (2019).
- [95] L. Pausch, E. G. Carnio, A. Rodríguez, and A. Buchleitner, Chaos and ergodicity across the energy spectrum of interacting bosons, *Phys. Rev. Lett.* **126**, 150601 (2021).
- [96] Y. Liu, P. Sierant, P. Stornati, M. Lewenstein, and M. Płodzień, Quantum algorithms for inverse participation ratio estimation in multiqubit and multiqudit systems, *Phys. Rev. A* **111**, 052614 (2025).
- [97] B. Eastin and E. Knill, Restrictions on transversal encoded quantum gate sets, *Physical Review Letters* **102**, 110502 (2009), arXiv:0811.4262 [quant-ph].
- [98] S. Bravyi and R. Koenig, Classification of topologically protected gates for local stabilizer codes, *Physi-*

- cal Review Letters **110**, 170503 (2013), arXiv:1206.1609 [quant-ph].
- [99] H. Bombín, Dimensional jump in quantum error correction, *New Journal of Physics* **18**, 043038 (2016), arXiv:1412.5079 [quant-ph].
- [100] X. Turkeshi, P. Calabrese, and A. D. Luca, Quantum mpemba effect in random circuits, *Phys. Rev. Lett.* **135**, 040403 (2025).
- [101] S. Liu, H.-K. Zhang, S.-X. Yin, and S.-X. Zhang, Symmetry restoration and quantum mpemba effect in symmetric random circuits, *Phys. Rev. Lett.* **133**, 140405 (2024).
- [102] S. Aditya, A. Summer, P. Sierant, and X. Turkeshi, Mpemba effects in quantum complexity (2025), arXiv:2509.22176 [quant-ph].
- [103] A. Summer, M. Moroder, L. P. Bettmann, X. Turkeshi, I. Marvian, and J. Goold, A resource theoretical unification of mpemba effects: classical and quantum (2025), arXiv:2507.16976 [quant-ph].
- [104] T. Haug and L. Piroli, Stabilizer entropies and nonstabilizerness monotones, *Quantum* **7**, 1092 (2023).
- [105] L. Leone and L. Bittel, Stabilizer entropies are monotones for magic-state resource theory, *Phys. Rev. A* **110**, L040403 (2024).
- [106] S. F. E. Oliviero, L. Leone, A. Hamma, and S. Lloyd, Measuring magic on a quantum processor, *npj Quantum Information* **8**, 148 (2022).
- [107] P. Niroula, C. D. White, Q. Wang, S. Johri, D. Zhu, C. Monroe, C. Noel, and M. J. Gullans, Phase transition in magic with random quantum circuits (2024).
- [108] T. Haug, S. Lee, and M. S. Kim, Efficient quantum algorithms for stabilizer entropies, *Phys. Rev. Lett.* **132**, 240602 (2024).
- [109] T. Haug and P. S. Tarabunga, Efficient witnessing and testing of magic in mixed quantum states, arxiv:2504.18098 (2025).
- [110] M. Heinrich and D. Gross, Robustness of magic and symmetries of the stabiliser polytope, *Quantum* **3**, 132 (2019).
- [111] H. Hamaguchi, K. Hamada, and N. Yoshioka, Handbook for Quantifying Robustness of Magic, *Quantum* **8**, 1461 (2024).
- [112] F. Levi and F. Mintert, A quantitative theory of coherent delocalization, *New Journal of Physics* **16**, 033007 (2014).
- [113] G. B. Mbeng, A. Russomanno, and G. E. Santoro, The quantum Ising chain for beginners, *SciPost Phys. Lect. Notes* , 82 (2024).
- [114] J. Surace and L. Tagliacozzo, Fermionic Gaussian states: an introduction to numerical approaches, *SciPost Phys. Lect. Notes* , 54 (2022).
- [115] I. Peschel and V. Eisler, Reduced density matrices and entanglement entropy in free lattice models, *Journal of Physics A: Mathematical and Theoretical* **42**, 504003 (2009).
- [116] J. Williamson, On the algebraic problem concerning the normal forms of linear dynamical systems, *Am. J. Math.* **58**, 141 (1936).
- [117] B. Zumino, Normal forms of complex matrices, *J. Math. Phys.* **3**, 1055 (1962).
- [118] See the supplementary material.
- [119] S. Aaronson and D. Gottesman, Improved simulation of stabilizer circuits, *Phys. Rev. A* **70**, 052328 (2004).
- [120] C. Gidney, Stim: a fast stabilizer circuit simulator, *Quantum* **5**, 497 (2021).
- [121] L. G. Valiant, Quantum computers that can be simulated classically in polynomial time, in *Proceedings of the Thirty-Third Annual ACM Symposium on Theory of Computing (STOC '01)* (Association for Computing Machinery, New York, NY, USA, 2001) pp. 114–123.
- [122] B. M. Terhal and D. P. DiVincenzo, Classical simulation of noninteracting-fermion quantum circuits, *Phys. Rev. A* **65**, 032325 (2002).
- [123] R. Jozsa and A. Miyake, Matchgates and classical simulation of quantum circuits, *Proc. R. Soc. A Math. Phys. Eng. Sci.* **464**, 3089–3106 (2008).
- [124] S. Bravyi and A. Kitaev, Universal quantum computation with ideal clifford gates and noisy ancillas, *Phys. Rev. A* **71**, 022316 (2005).
- [125] M. Oszmaniec, N. Dangniam, M. E. Morales, and Z. Zimborás, Fermion sampling: A robust quantum computational advantage scheme using fermionic linear optics and magic input states, *PRX Quantum* **3**, 020328 (2022).
- [126] L. Ebner, B. Müller, A. Schäfer, L. Schmotzer, C. Seidl, and X. Yao, The magic barrier before thermalization (2025), arXiv:2510.11681 [quant-ph].
- [127] E. Tirrito, P. S. Tarabunga, G. Lami, T. Chanda, L. Leone, S. F. E. Oliviero, M. Dalmonte, M. Collura, and A. Hamma, Quantifying nonstabilizerness through entanglement spectrum flatness, *Phys. Rev. A* **109**, L040401 (2024).
- [128] C. Cao, G. Cheng, A. Hamma, L. Leone, W. Munnizzi, and S. F. E. Oliviero, Gravitational back-reaction is magical, arXiv preprint 10.48550/arXiv.2403.07056 (2025), arXiv:2403.07056 [hep-th].
- [129] S. Bravyi and D. Gosset, Improved classical simulation of quantum circuits dominated by clifford gates, *Physical Review Letters* **116**, 250501 (2016), arXiv:1601.07601 [quant-ph].
- [130] S. Bravyi, D. Browne, P. Calpin, E. Campbell, D. Gosset, and M. Howard, Simulation of quantum circuits by low-rank stabilizer decompositions, *Quantum* **3**, 181 (2019).
- [131] V. Khemani, A. Vishwanath, and D. A. Huse, Operator spreading and the emergence of dissipative hydrodynamics under unitary evolution with conservation laws, *Physical Review X* **8**, 031057 (2018), arXiv:1710.09835 [cond-mat.stat-mech].
- [132] T. Rakovszky, F. Pollmann, and C. W. von Keyserlingk, Sub-ballistic growth of rényi entropies due to diffusion, *Physical Review Letters* **122**, 250602 (2019), arXiv:1901.10502 [cond-mat.stat-mech].
- [133] A. A. Michailidis, D. A. Abanin, and L. V. Delacrétaz, Corrections to diffusion in interacting quantum systems, *Physical Review X* **14**, 031020 (2024), arXiv:2310.10564 [cond-mat.stat-mech].
- [134] Y. Zhang and Y. Gu, Quantum magic dynamics in random circuits, arXiv preprint 10.48550/arXiv.2410.21128 (2024), arXiv:2410.21128 [quant-ph].
- [135] R. Moessner and S. L. Sondhi, Equilibration and order in quantum floquet matter, *Nature Physics* **13**, 424 (2017).
- [136] A. Polkovnikov, K. Sengupta, A. Silva, and M. Vengalattore, Colloquium: Nonequilibrium dynamics of closed interacting quantum systems, *Rev. Mod. Phys.* **83**, 863 (2011).
- [137] L. Vidmar and M. Rigol, Generalized gibbs ensemble in

- integrable lattice models, *Journal of Statistical Mechanics: Theory and Experiment*, 064007 (2016).
- [138] M. Serbyn, D. A. Abanin, and Z. Papić, Quantum many-body scars and weak breaking of ergodicity, *Nature Physics* **17**, 675 (2021).
- [139] A. Chandran, T. Iadecola, V. Khemani, and R. Moessner, Quantum many-body scars: A quasiparticle perspective, *Annual Review of Condensed Matter Physics* **14**, 443 (2023).
- [140] X. Turkeshi, A. Dymarsky, and P. Sierant, Pauli spectrum and nonstabilizerness of typical quantum many-body states, *Phys. Rev. B* **111**, 054301 (2025).
- [141] S. Maity and R. Hamazaki, Local spreading of stabilizer rényi entropy in a brickwork random clifford circuit (2025), arXiv:2511.07769 [quant-ph].
- [142] M. Bejan, P. W. Claeys, and J. Yao, Magic spreading under unitary clifford dynamics (2025), arXiv:2511.21487 [quant-ph].
- [143] D. Gross, Hudson's theorem for finite-dimensional quantum systems, *Journal of Mathematical Physics* **47**, 122107 (2006).
- [144] V. Veitch, C. Ferrie, D. Gross, and J. Emerson, Negative quasi-probability as a resource for quantum computation, *New J. Phys.* **14**, 113011 (2012).
- [145] P. S. Tarabunga, Critical behaviors of non-stabilizerness in quantum spin chains, *Quantum* **8**, 1413 (2024).
- [146] D. Gottesman, Fault-tolerant quantum computation with higher-dimensional systems, *Chaos, Solitons & Fractals* **10**, 1749 (1999).

Supplemental Material for Growth and spreading of quantum resources under random circuit dynamics

Sreemayee Aditya, Xhek Turkeshi, Piotr Sierant

Subsystem-size dependence of resource-monotone decay times.— As discussed in the Main Text, the resource monotones, under resource generating dynamics, at late times relax exponentially toward the local maximally mixed state. Here, we quantify this decay using two complementary approaches. First, we fit the late-time profiles of resource monotones to exponentially decaying functions to extract the corresponding decay times and study their dependence on the subsystem size L_A . Second, we employ a threshold-based characterization of the decay time by defining a threshold time τ_θ such that for $t > \tau_\theta$ the resource measures fulfill $M(\rho_A(t)) < \theta \ll 1$, and we examine how τ_θ scales with L_A .

Restricting to the first setup of the Main Text, i.e., resourceful dynamics initialized in an initially resourceless state, we examine the late-time decay of the local resource content for three resource quantifiers: non-stabilizerness (a), coherence (b), and non-Gaussianity (c). Fitting the long time decays of monotones respectively with $\mathcal{L}(\rho_A(t)) \propto e^{-t/\tau_L^d}$, $C_d(\rho_A(t)) \propto e^{-t/\tau_c^d}$, and $\mathcal{N}\mathcal{G}(\rho_A(t)) \propto e^{-t/\tau_N^d}$, we extract the decay constants τ_R^d (with $R = \mathcal{L}, c, N$). We obtain $\tau_L^d = (9.42, 9.30, 9.50)$ for $L_A = (2, 3, 4)$ (non-stabilizerness), $\tau_c^d = (9.90, 10.01, 9.65)$ for $L_A = (8, 12, 16)$ (coherence), and $\tau_N^d = (7.20, 7.33, 7.48, 7.42, 7.46)$ for $L_A = (8, 16, 24, 32, 36)$ (non-Gaussianity). Across all three diagnostics, the extracted τ_R^d values fluctuate by at most $\sim 5\%$ over the explored range of L_A , indicating that to an essentially subsystem-size-independent late-time decay.

In Fig. S1, we turn to the threshold timescale τ_θ for the same setup and the same three resources. Here the behavior is markedly different: τ_θ increases linearly with L_A , indicating $\tau_\theta \propto L_A$. Taken together, these observations point to a clear separation of dynamical regimes. The scaling $\tau_\theta \propto L_A$ is consistent with ballistic propagation of correlations, where the onset of resource depletion is set by a light-cone traversal across a subsystem of size L_A . By contrast, the subsequent late-time relaxation is governed by local dynamics, leading to an exponential decay of the resource monotones with an L_A -independent timescale τ_d . In this sense, the ballistic spreading controls the *onset* of resource depletion, while the *rate* of the asymptotic decay is determined by a local equilibration process.

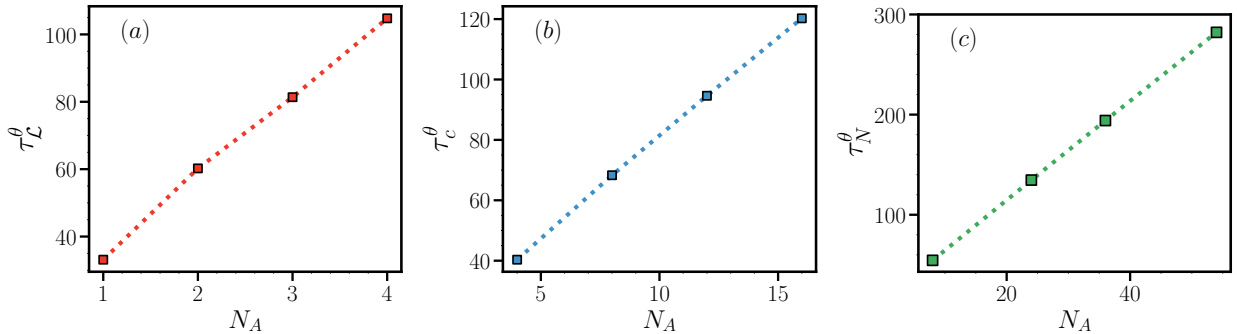


Figure S1. Subsystem-size dependence of the threshold time τ_θ for three representative resource measures: (a) non-stabilizerness ($L = 24$ qubits), (b) coherence ($L = 128$ qubits), and (c) non-Gaussianity ($L = 128$ qubits). Starting from a resourceless initial state, the system evolves under resourceful dynamics generated by two-qubit operations for the setup shown in Fig. 2 in the main text. We define τ_θ implicitly by the threshold condition $M(\tau_\theta) = \theta$, with θ fixed to 0.01 for nonstabilizerness and to 0.1 for coherence and non-Gaussianity. Across all three measures, τ_θ grows linearly with the subsystem size L_A .